

Neutral “Cp-Free” Silyl-Lanthanide(II) Complexes: Synthesis, Structure, and Bonding Analysis

Rainer Zitz,[†] Johann Hlina,[‡] Karl Gatterer,[§] Christoph Marschner,[†] Tibor Szilvási,^{*,||} and Judith Baumgartner^{*,‡}

[†]Institut für Anorganische Chemie, Technische Universität Graz, Stremayrgasse 9, 8010 Graz, Austria

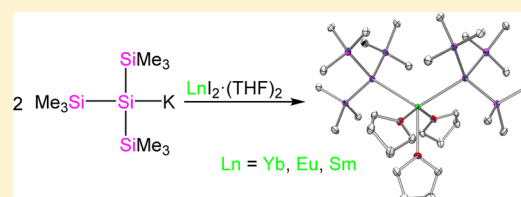
[‡]Institut für Chemie, Universität Graz, Stremayrgasse 9, 8010 Graz, Austria

[§]Institut für Physikalische und Theoretische Chemie, Technische Universität Graz, Stremayrgasse 9, 8010 Graz, Austria

^{||}Department of Inorganic and Analytical Chemistry, Budapest University of Technology and Economics (BUTE), Szent Gellért tér 4, 1111 Budapest, Hungary

S Supporting Information

ABSTRACT: Complexes featuring lanthanide silicon bonds represent a research area still in its infancy. Herein, we report a series of Cp-free lanthanide (+II) complexes bearing σ -bonded silyl ligands. By reactions of LnI_2 ($\text{Ln} = \text{Yb}, \text{Eu}, \text{Sm}$) either with a 1,4-oligosilanyl dianion $[\text{K}-\text{Si}(\text{SiMe}_3)_2\text{SiMe}_2\text{SiMe}_2\text{Si}(\text{SiMe}_3)_2-\text{K}]$ (**1**) or with **2** $(\text{Me}_3\text{Si})_3\text{SiK}$ (**3**) the corresponding neutral metallacyclopentasilanes ($\{\text{Me}_2\text{Si}(\text{Me}_3\text{Si})_2\text{Si}\}_2\text{Ln} \cdot (\text{THF})_4$ ($\text{Ln} = \text{Yb}$ (**2a**), Eu (**2b**), Sm (**2c**)), or the disilylated complexes ($\{\text{Me}_3\text{Si}\}_3\text{Si}\}_2\text{Ln} \cdot (\text{THF})_3$ ($\text{Ln} = \text{Yb}$ (**4a**), Eu (**4b**), Sm (**4c**))), were selectively obtained. Complexes **2b**, **2c**, **4b**, and **4c** represent the first examples of structurally characterized Cp-free Eu and Sm complexes with silyl ligands. In both series, a linear correlation was observed between the Ln–Si bond lengths and the covalent radii of the corresponding lanthanide metals. Density functional theory calculations were also carried out for complexes **2a–c** and **4a–c** to elucidate the bonding situation between the Ln(+II) centers and Si.



INTRODUCTION

Complexes with the metal in the oxidation state 3+ bearing Cp or substituted Cp ligands are dominating the organometallic chemistry of the rare-earth elements. With respect to the divalent oxidation state,^{1,2} for a long time only three lanthanide elements, samarium, europium, and ytterbium, were readily accessible. However, in the meantime the number of elements has increased substantially, and quite recently Evans et al. were successful in completing the series of crystalline examples of divalent molecular complexes of all lanthanides.^{3–6} This enabled for the first time a comparison of all lanthanides in a single uniform coordination environment and postulation of their electronic ground states.⁶ The results show conclusively that ligands can change the electronic ground state of Ln(II) complexes whereas this has not been observed for the Ln(III) complexes. Due to the high energy of the 5d orbitals and the limited radial extensions of the 4f orbitals for Ln(III) complexes, interactions with the ligands are weaker.⁶

Although numerous examples of d-block metal-silyl compounds exist, examples of rare-earth metal-silyl compounds are still scarce or entirely unknown for some elements. The few reported samarium silyl compounds, which have also been characterized by X-ray diffraction analysis, feature Sm with Cp* ligands almost exclusively in oxidation state 3+^{7–9} with the exception of some divalent silylene complexes reported by Evans and co-workers¹⁰ and our group.¹¹ The reaction of $\text{Cp}^*_2\text{Yb} \cdot (\text{Et}_2\text{O})$ with $(\text{Me}_3\text{Si})_3\text{SiLi}$ was shown to result in the

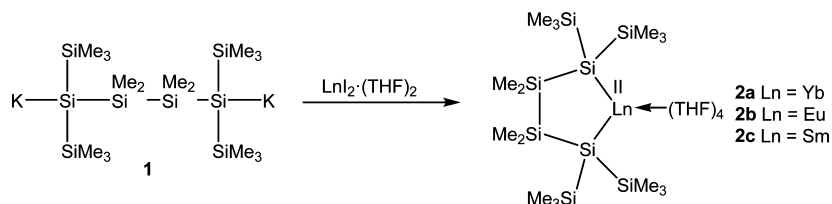
formation of $\text{Cp}^*_2\text{YbSi}(\text{SiMe}_3)_3 \cdot (\text{THF})_2$ accompanied by elimination of Cp^*_2Li .¹² Reacting $\text{Cp}^*_2\text{YbSi}(\text{SiMe}_3)_3 \cdot (\text{THF})_2$ with excess $(\text{Me}_3\text{Si})_3\text{SiLi}$ led to the formation of some 30% of $[(\text{Me}_3\text{Si})_3\text{Si}]_2\text{Yb} \cdot (\text{THF})_x$, which could not be isolated.¹² The reaction of $\text{Cp}^*_2\text{Ln} \cdot (\text{THF})_2$ ($\text{Ln} = \text{Sm}, \text{Eu}, \text{Yb}$) with PhSiH_3/KH , which yields metalate complexes of the type $\text{K}[\text{Cp}^*_2\text{Ln}^{\text{II}}(\text{SiH}_3) \cdot (\text{THF})]$,¹³ also seems to involve silyl anions. The respective Eu and Yb complexes could be successfully characterized using single crystal X-ray diffraction analysis. In addition Bochkarev and co-workers reported the synthesis of neutral Cp-free $(\text{Ph}_3\text{Si})_2\text{Yb}^{\text{II}}(\text{THF})_4$ by direct treatment of elemental ytterbium with Ph_3SiCl in THF.¹⁴

Divalent rare-earth amides, particularly silylamides $[\text{Ln}^{\text{II}}\text{N}(\text{SiMe}_3)_2]$, have also received some attention.^{15–18} A few of these compounds do not contain cyclopentadienyl ligands on the metal and are therefore interesting for the exploration of catalytic processes such as hydrosilylation¹⁹ or enantioselective hydroamination²⁰ and polymerization of polar monomers like methyl methacrylate and lactones.²¹ Recently, Evans et al. could show reactions of N_2 , CO, and CO_2 with $[(\text{Me}_3\text{Si})_2\text{N}]_3\text{Ln}$ complexes, where N_2 is reduced to $(\text{N}=\text{N})^{2-}$ and $(\text{N}_2)^{3-}$ and CO and CO_2 are reduced to the rare $(\text{CO})^{1-}$ and $(\text{CO}_2)^{1-}$ radicals.^{4,22} Despite the lack of direct Ln–Si bonds, β -agostic interactions^{23,24} play an important role in lanthanide complexes

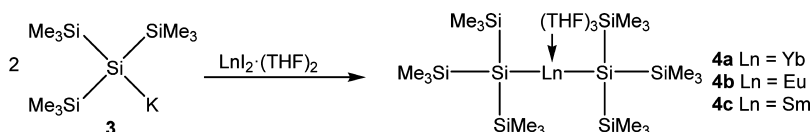
Received: May 14, 2015

Published: July 1, 2015

Scheme 1. Preparation of Lanthanide Oligosilanyl Complexes 2a–c



Scheme 2. Synthesis of Lanthanide Oligosilanyl Complexes 4a–c



that contain the $\text{N}(\text{SiMe}_2\text{H})_2$ group.¹⁸ Several types of agostic lanthanide hydridosilylamido complexes^{25,26} have been prepared employing $[\text{N}(\text{SiMe}_2\text{H})_2]$ and $[t\text{BuN}(\text{SiMe}_2\text{H})]$ ligands,^{18,27} and with the use of density functional theory (DFT) calculations their role as ligands was examined.²⁵ In a recent example, Niemeyer reacted divalent $[\text{Yb}^{\text{II}}\{\text{N}(\text{SiMe}_3)_2\}_2]$ with $(\text{Me}_3\text{Si})_3\text{SiK}$ to afford $\text{K}[(\text{Me}_3\text{Si})_3\text{SiYb}^{\text{II}}\{\text{N}(\text{SiMe}_3)_2\}_2]$.^{28,29} In sharp contrast, reaction of the respective trivalent $[\text{Yb}^{\text{III}}\{\text{N}(\text{SiMe}_3)_2\}_3]$ with $\text{KSi}(\text{SiMe}_3)_3$ led to methyl deprotonation of a trimethylsilyl group rather than to $\text{Si}-\text{Yb}^{\text{III}}$ bond formation.^{28,29}

β -Agostic interactions are important not only in complexes with $\text{N}(\text{SiMe}_2\text{H})_2$ groups but also in complexes like $\text{Yb}[\text{C}(\text{SiMe}_2\text{H})_3]_2\cdot\text{THF}_2$ ³⁰ or $\text{Yb}[\text{C}(\text{SiMe}_2\text{H})_3]_2\cdot\text{TMEDA}$ ³¹ containing the $\text{C}(\text{SiMe}_2\text{H})_3$ ligand. The short $\text{Yb}-\text{Si}$ distances as well as the small $\text{Yb}-\text{C}-\text{Si}$ angles in the crystal structure are in perfect concordance with the β -agostic $\text{Si}-\text{H}-\text{Yb}$ interactions.^{30,31}

We recently reported synthesis and characterization of some σ -bonded Cp_2 -lanthanide-silyl complexes ($\text{Ln} = \text{Tm}, \text{Ho}, \text{Gd}, \text{Tb}, \text{Ce}$) in the oxidation state 3+.¹¹ Herein, the synthesis of Cp-free samarium-, europium-, and ytterbium-silyl complexes in the oxidation state 2+ are described in addition to a thorough investigation into their spectroscopic properties, X-ray diffraction studies, and the first systematic density functional theory (DFT) investigation for this class of complexes.

RESULTS AND DISCUSSION

Synthesis. Ytterbium(II), europium(II), and samarium(II) diiodides were investigated with regard to their reactivity with oligosilanyl anions. The THF complexes $\text{LnI}_2\cdot(\text{THF})_2$ [$\text{Ln} = \text{Yb}$ (yellow), Eu (dark yellow), Sm (dark blue)] were prepared by reaction of small pieces of metal with 1,2-diiodoethane in THF.^{32,33} The dark blue $\text{SmI}_2\cdot(\text{THF})_2$ was either dissolved in THF or suspended in toluene and treated with silanyl mono- or dianions. Using the less reactive silyl magnesium compounds $[(\text{Me}_3\text{Si})_3\text{Si}]_2\text{Mg}$ ³⁴ or $[\text{Me}_2\text{Si}(\text{Me}_3\text{Si})_2\text{Si}]_2\text{Mg}$ ³⁴ did not cause any reaction at ambient temperature within 18 h as judged by *in situ* ^1H and ^{29}Si NMR spectroscopy, and the solutions remained dark blue. In addition, heating the reaction mixture to 80 °C for 3 h did not lead to any observable changes. With the more reactive system $(\text{Me}_3\text{Si})_3\text{SiK}\cdot 18\text{-crown-6}$ ³⁵ in toluene only the formation of $(\text{Me}_3\text{Si})_2\text{Si}$ could be observed. The formation of $(\text{Me}_3\text{Si})_2\text{Sm}\cdot(\text{THF})_x$ had been reported to occur in the reaction of hexamethyldisilane with samarium amalgam leading to an inseparable mixture of the desired $\text{Sm}(\text{II})$ compound and

$\text{Sm}(\text{III})$ derivatives.³⁶ It was further proposed that reaction at low temperature and large excess of samarium would lead to a more selective reaction to the $\text{Sm}(\text{II})$ complex.³⁶ Eventually, we tried the treatment of $\text{SmI}_2\cdot(\text{THF})_2$ in THF with $[\text{Me}_2\text{Si}(\text{Me}_3\text{Si})_2\text{Si}]_2\text{K}$ (1) or 2 equiv of $(\text{Me}_3\text{Si})_3\text{SiK}$ (3) and obtained dark violet reaction mixtures. Reaction monitoring by ^1H and ^{29}Si NMR spectroscopy showed the formation of $[\text{Me}_2\text{Si}(\text{Me}_3\text{Si})_2\text{Si}]_2\text{Sm}\cdot(\text{THF})_4$ (2c) (Scheme 1) and $[(\text{Me}_3\text{Si})_3\text{Si}]_2\text{Sm}\cdot(\text{THF})_3$ (4c) (Scheme 2), respectively. Both compounds could be isolated as very air and moisture sensitive but stable crystalline compounds.

With this success, we reasoned that the synthesis of analogous ytterbium complexes might be accomplished in a similar manner. Monitoring the reaction of 3 with $\text{YbI}_2\cdot(\text{THF})_2$ by NMR spectroscopy showed after only 15 min complete consumption of starting material 3 and the formation of 4a along with substantial amounts of tetrakis(trimethylsilyl)silane and tris(trimethylsilyl)silane. In an analogous manner, reaction of $\text{YbI}_2\cdot(\text{THF})_2$ with 1 showed formation of 2a, but again the generation of several side products was observed. These results are similar to what was previously described for titanium³⁷ and yttrium³⁸ complexes bearing tris(trimethylsilyl)silyl groups. The problem could be overcome by strict exclusion of light during the formation and storage of 2a and 4a. Exposure of 2a to ambient light over the duration of a week caused decomposition to 1,1,2,2-tetrakis(trimethylsilyl)-tetramethylcyclotetrasilane³⁹ as the main product. The yields of 2a and 4a could be increased by changing the solvent from THF to toluene or DME (2a·DME). Both 2a and 4a are not only light sensitive but also extremely air and moisture sensitive. Exposing 2a to vacuum over several hours resulted in complete decomposition of the complex and in generation of 1,1,4,4-tetrakis(trimethylsilyl)tetrasilane and uncharacterizable insoluble metal species.

The synthesis of the europium compounds 2b and 4b turned out to be similar to the ytterbium complexes. Again, selective reactions with short reaction time were observed in toluene, and air and moisture sensitive crystalline compounds were obtained.

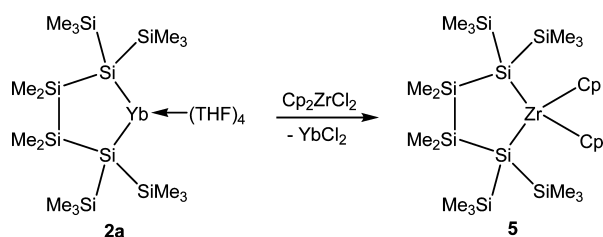
Reaction of LnI_2 ($\text{Ln} = \text{Yb}, \text{Eu}, \text{or Sm}$) according to Scheme 2 with just 1 equiv of silyl anion 3 led in all our attempts only to products 4a–c, and no evidence for the formation of a monosilylated complex $(\text{Me}_3\text{Si})_3\text{SiLnI}$ was found.

The determination of yields of all compounds was somewhat hampered by some loss of THF during the isolation process due to the use of reduced pressure. For the diamagnetic Yb

compound **2a** the yield could however be determined NMR spectroscopically by using a defined amount of toluene as internal standard.

To get an estimate of the reactivity of the Si–Yb bond of **2a** a reaction with Cp_2ZrCl_2 was carried out. The analogous reactions with the potassium or magnesium 1,4-disilanes^{34,40,41} are known to give the respective zirconacyclopentasilane (**5**).^{40,41} The same course was also observed in the reaction of **2a** with Cp_2ZrCl_2 (Scheme 3). This outcome certainly marks compound **2a** as possessing a strong disilanide character.

Scheme 3. Preparation of a Zirconacyclopentasilane 5 from Yb Complex 2a



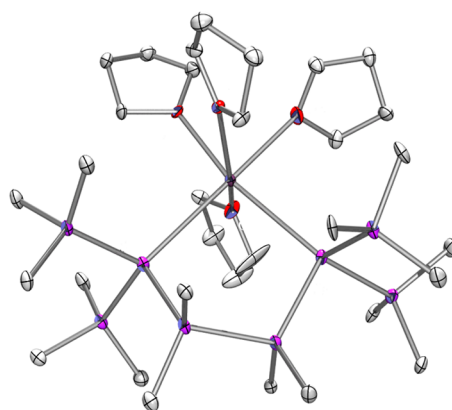
NMR Spectroscopy. With respect to NMR spectroscopy, the diamagnetic ytterbium complexes **2a** and **4a** are the most interesting ones with respect to insight into the bonding situation. While for the europium complexes **2b** and **4b** no meaningful NMR spectra could be obtained at all, the samarium complex **2c** and **4c** exhibited spectra with paramagnetically shifted signals.

So far two examples of tris(trimethylsilyl)silylated ytterbium(II) complexes are known. The neutral complex $\text{Cp}^*\text{YbSi}(\text{SiMe}_3)_3 \cdot (\text{THF})_2$,¹² reported by Lawless and co-workers, displays ²⁹Si NMR signals at -158.3 ppm (Yb–Si) and -2.9 ppm ($\text{Si}(\text{SiMe}_3)_3$) with a Si–Yb coupling constant of $^1J_{\text{Si–Yb}} = 829$ Hz. The respective signals of Niemeyer’s ate-complex $\text{K}[(\text{Me}_3\text{Si})_3\text{SiYb}\{\text{N}(\text{SiMe}_3)_2\}_2]$ ²⁸ are similar to resonances at -148.6 ppm (Yb–Si) and -4.7 ppm ($\text{Si}(\text{SiMe}_3)_3$) and a somewhat smaller Yb–Si coupling constant ($^1J_{\text{Si–Yb}} = 716$ Hz). The ²⁹Si NMR spectrum of **4a** is quite similar to Niemeyer’s complex with signals at -144.8 and -5.3 ppm and visible ¹⁷¹Yb satellites for the central silicon signal in the ²⁹Si INEPT spectrum with a coupling constant of $^1J_{\text{Si–Yb}} = 732$ Hz. The ²⁹Si NMR spectrum of the ytterbacyclopentasilane **2a** in C_6D_6 shows an upfield shift for the metalated silicon atoms to a value of -154.0 ppm with the Yb–Si coupling constant not determinable. The signals for the SiMe_2 (-30.5 ppm) and SiMe_3 (-3.5 ppm) groups are within the range of expectation. Very similar spectroscopic data were also found for the analogous DME complex **2a**·DME with signals at -158.4 ppm ($^1J_{\text{Yb–Si}} = 656$ Hz, $\text{Si}(\text{SiMe}_3)_3$), -29.8 ppm (SiMe_2), and -2.9 ppm ($^2J_{\text{Yb–Si}} = 20.4$ Hz, SiMe_3). When the formation of **2a** was carried out directly in C_6D_6 instead of toluene with an approximate THF concentration of 9 equiv per Yb atom, the ²⁹Si NMR spectrum of the reaction solution indicated a higher degree of shielding of the metalated silicon atom with the resonance shifted to -163.9 ppm and a $^1J_{\text{Yb–Si}}$ coupling constant of 633 Hz. The substantial shift from -154.0 to -163.0 ppm suggests a higher degree of solvation of the Yb atom in the presence of THF.

A comparison of the ²⁹Si NMR spectroscopic data with structurally related compounds such as analogous magnesium,

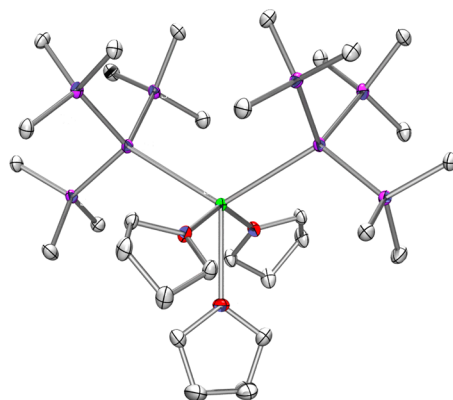
zinc, zirconocene, and hafnocene complexes helps to obtain some insight into the nature of the Si–Yb interaction. The oligosilylanyl magnesium compounds $[(\text{Me}_3\text{Si})_3\text{Si}]_2\text{Mg} \cdot (\text{THF})_2$,⁴² [$\delta^{29}\text{Si} = -171.9$ ppm (SiMg), -6.4 ppm (SiMe₃)], $[(\text{Me}_3\text{Si})_3\text{Si}]_2\text{Mg} \cdot (\text{TMEDA})$,³⁴ [$\delta^{29}\text{Si} = -170.2$ ppm (SiMg), -7.5 ppm (SiMe₃)], and $[\text{Me}_2\text{Si}(\text{Me}_3\text{Si})_2\text{Si}]_2\text{Mg} \cdot (\text{THF})_2$,³⁴ [$\delta^{29}\text{Si} = -176.6$ ppm (SiMg), -27.1 ppm (SiMe₂), -5.4 ppm (SiMe₃)] which are quite ionic compounds feature the chemical shift of the metalated silicon atoms at higher field than **2a** and **4a**. This is in sharp contrast to the zirconium compounds $[(\text{Me}_3\text{Si})_3\text{Si}]_2\text{ZrCp}_2$,⁴³ [$\delta^{29}\text{Si} = -83.9$ ppm (SiZr), -6.7 ppm (SiMe₃)] and $[\text{Me}_2\text{Si}(\text{Me}_3\text{Si})_2\text{Si}]_2\text{ZrCp}_2$,^{40,41} [$\delta^{29}\text{Si} = -65.2$ ppm (SiZr), -29.2 ppm (SiMe₂), -2.4 ppm (SiMe₃)] and the hafnium compounds $[(\text{Me}_3\text{Si})_3\text{Si}]_2\text{HfCp}_2$,⁴³ [$\delta^{29}\text{Si} = -82.4$ ppm (SiHf), -8.2 ppm (SiMe₃)], $[\text{Me}_2\text{Si}(\text{Me}_3\text{Si})_2\text{Si}]_2\text{HfCp}_2$,⁴¹ [$\delta^{29}\text{Si} = -52.2$ ppm (SiZr), -27.8 ppm (SiMe₂), -2.0 ppm (SiMe₃)], and $(\text{Me}_3\text{Si})_3\text{SiHfCl}_3 \cdot (\text{TMEDA})$,⁴⁴ [$\delta^{29}\text{Si} = -56.3$ ppm (SiHf), -2.6 ppm (SiMe₃)], which display chemical shifts of the metalated silicon atoms considerably downfield, which is consistent with a much higher degree of covalent bonding. The closest analogues with respect to the chemical shifts of the metalated silicon atoms are the silyl zinc compounds $[(\text{Me}_3\text{Si})_3\text{Si}]_2\text{Zn}$,⁴⁵ [$\delta^{29}\text{Si} = -123.9$ ppm (SiZn), -8.2 ppm (SiMe₃)], $[(\text{Me}_3\text{Si})_3\text{Si}]_2\text{Zn} \cdot (\text{bipy})$,⁴⁵ [$\delta^{29}\text{Si} = -150.8$ ppm (SiZr), -6.6 ppm (SiMe₃)], $(\text{Me}_3\text{Si})_3\text{SiZnCl} \cdot (\text{TMEDA})$,⁴⁶ [$\delta^{29}\text{Si} = -156.8$ ppm (SiZr), -8.0 ppm (SiMe₃)], and $\text{K}[\text{Me}_2\text{Si}(\text{Me}_3\text{Si})_2\text{Si}]_2\text{ZnCl}$,⁴⁶ [$\delta^{29}\text{Si} = -152.1$ ppm (SiZr), -26.6 ppm (SiMe₂), -6.3 ppm (SiMe₃)]. Another aspect that makes a comparison with oligosilylanyl zinc compounds tempting is the observed upfield shift for a distorted geometry at Zn from $\delta = -123.9$ ppm for the linear Si–Zn–Si arrangement in $[(\text{Me}_3\text{Si})_3\text{Si}]_2\text{Zn}$ ⁴⁵ to $\delta = -150.8$ ppm for the bent Si–Zn–Si arrangement in $[(\text{Me}_3\text{Si})_3\text{Si}]_2\text{Zn} \cdot (\text{bipy})$.⁴⁵ For the Si–Yb–Si complexes **4a** and **2a** a similar behavior can be observed, where the shift of the undistorted complex **4a** of $\delta = -144.8$ ppm is raised to $\delta = -154.0$, -158.5 ppm for the constrained geometry of complexes **2a** and **2a**·DME with much smaller Si–Yb–Si angles than found for **4a**. From these NMR data it seems likely that the polarization of the Si–Yb bond should be somewhat more pronounced than that of a Si–Zn bond but less than a Si–Mg bond. This conclusion seems to be consistent with the reaction of **2a** with Cp_2ZrCl_2 to **5** which also hints at a high degree of polarization.

The number of silylated samarium complexes with elucidated crystal structures is scant,^{7–10,47} and only for one compound, $\text{Cp}^*\text{SmSiH}(\text{SiMe}_3)_2$, are ²⁹Si NMR spectroscopic data known ($\delta^{29}\text{Si} = -23.5$ ppm (SiMe₃), no signal detected for Si–Sm).^{7,8} None of the known complexes for which NMR spectroscopic data are given features Sm in the oxidation state 2+. However, a comparison of the NMR spectroscopic properties of Cp^*_3Sm ⁴⁸ and $\text{Cp}^*_2\text{Sm} \cdot (\text{THF})_2$ ⁴⁹ provides some ideas as to what to expect for the NMR spectra of **2c** and **4c**. The ¹³C NMR resonances for the Cp* unit were found for Cp^*_3Sm at $\delta = 113.2$ ppm (C_5Me_5) and 28.3 ppm (C_5Me_5) while for $\text{Cp}^*_2\text{Sm} \cdot (\text{THF})_2$ these signals were found at $\delta = -73.7$ ppm (C_5Me_5) and 94.6 ppm (C_5Me_5). The THF resonances for $\text{Cp}^*_2\text{Sm} \cdot (\text{THF})_2$ were found at $\delta = 149.5$ ppm (OCH₂) and 33.4 ppm (OCH₂CH₂). It seems thus reasonable to expect ²⁹Si NMR shifts for **2c** and **4c** to be different from those of Sm^{III}–Si compounds. For the cyclic compound **2c** the ¹H NMR resonances were found to be not too much off the typical values with signals at $\delta = 4.60$ and 0.65 ppm for coordinating



2a	2b	2c
yellow crystals	yellow crystals	green crystals
space group: P2(1)/n	space group: R-3	space group: P2(1)/n
Si-Yb: 3.106, 3.171 Å	Si-Eu: 3.2052, 3.2162 Å	Si-Sm: 3.2132, 3.2444 Å
O-Yb: 2.433 - 2.485 Å	O-Eu: 2.546 - 2.613 Å	O-Sm: 2.544 - 2.613 Å
Si-Yb-Si 91.92°	Si-Eu-Si 91.09°	Si-Sm-Si 89.16°

Figure 1. Some key metrical parameters from the crystal structures of the isostructural complexes **2a–c**. Thermal ellipsoids at the 30% probability level and hydrogen atoms omitted for clarity. Color code: brown = lanthanide metal (Yb (**2a**), Eu (**2b**), Sm (**2c**)), pink = silicon, light gray = carbon.



4a	4b	4c
yellow crystals	yellow crystals	red crystals
space group: Pbcn	space group: Pna2(1)	space group: Pbcn
Si-Yb: 3.0644 Å	Si-Eu: 3.1497 Å	Si-Sm: 3.1716 Å
O-Yb: 2.421 - 2.435 Å	O-Eu: 2.515 - 2.524 Å	O-Sm: 2.551 - 2.528 Å
Si-Yb-Si 124.51°	Si-Eu-Si 122.53°	Si-Sm-Si 123.296°

Figure 2. Some key metrical parameters from the crystal structures of the isostructural complexes **4a–4c**. Thermal ellipsoids at the 30% probability level and hydrogen atoms omitted for clarity. Color code: green = lanthanide metal (Yb (**4a**), Eu (**4b**), Sm (**4c**)), pink = silicon, light gray = carbon.

THF and at $\delta = 0.53$ and -1.23 ppm for the SiMe_3 and SiMe_2 groups, respectively. The ^{13}C NMR signals at $\delta = 127.32$ and 25.35 ppm for coordinating THF are similar to that of $\text{Cp}^*\text{Sm}(\text{THF})_2$. Signals for $\text{Si}(\text{CH}_3)_2$ and $\text{Si}(\text{CH}_3)_3$ were observed at -14.49 and -18.20 ppm, respectively. The ^{29}Si signals are again typical for spatially defined atoms. The resonance for the SiMe_2 downfield shifted to $\delta = 120.9$ ppm whereas the SiMe_3 resonance at $\delta = -98.3$ ppm is upfield shifted. The chemical shift of the metalated Si atom at $\delta = -121.1$ seems to be least shifted compared to the values found for **2a** and **4a**. The spectroscopic features of the bis[tris(trimethylsilyl)silylated] **4c**

are similar to those of **4a** with similar ^1H NMR signals for THF of $\delta = 3.17$ and -0.90 ppm and a conspicuously normal trimethylsilyl resonance at $\delta = 0.04$ ppm. In the ^{13}C NMR spectrum THF signals appear at $\delta = 127.2$ and 21.8 ppm while the trimethylsilyl resonance was found at $\delta = -13.40$ ppm. In the ^{29}Si NMR spectrum only a resonance for the SiMe_3 groups was detected at $\delta = -27.4$ ppm. The comparably normal chemical shifts for the trimethylsilyl groups in the ^1H , ^{13}C , and ^{29}Si NMR spectra are likely caused by averaging the more extreme signals for **4c** by rotation around the Si–Sm and Si–Si bonds.

Fluorescence Spectroscopy. Among the divalent rare-earth ions, Eu^{2+} has attracted increasing attention over the past decades for its unique fluorescence properties.^{50,51} In $\text{Eu}^{3+}(4f^6)$ the emission after short wavelength excitation consists of relatively sharp $f-f$ bands found always at the same wavelengths. In contrast the corresponding emission of $\text{Eu}^{2+}(4f^7)$ is much broader, and depending on the material, it can occur at wavelengths in the blue, green, or red⁵² part of the visible spectrum. This is due to the $4f^65d^1 \rightarrow 4f^7$ nature of the Eu^{2+} emission. It is parity allowed and originates from the first excited state configuration, which involves $5d$ orbitals. Since the energy of the d -orbitals is strongly influenced by the surrounding crystal field, the transition can occur at different wavelengths in different Eu^{2+} containing materials.

The fluorescence spectrum of solid compound **4b** upon excitation at 366 nm shows a broad emission with a maximum intensity at 490 nm in the blue/green wavelength range (Supporting Information Figure S24). The fluorescence is strong enough to be seen with the naked eye. After a few minutes in the spectrometer's sample holder, however, the yellow sample in the central region of the sample holder, where it is hit by the excitation UV light, turns black indicating its decay. As expected a comparison with the fluorescence spectrum of solid $\text{EuI}_2(\text{THF})_2$ ⁵³ (Supporting Information Figure S24) reveals that the silyl groups are stronger crystal field ligands than iodide (Supporting Information Figure S25).

X-ray Crystallography. Molecular structures of all compounds **2a–c** (Figure 1) and **4a–c** (Figure 2) in the solid state could be determined by means of single crystal X-ray diffraction. Interestingly, neutral metallacyclopentasilanes **2a** and **2c** were found to crystallize in the monoclinic space group $P2_1/n$ whereas **2b** prefers the trigonal space group $R\bar{3}$. The difference in the space group is caused by a different packing pattern of **2b**. Within the crystal of complex **2b**, channels with a diameter of 13.62 Å are formed by an alternative arrangement of CH_3 units from the SiMe_3 groups and the CH_2 groups of the coordinate THF molecules. Compounds **2a–c** all contain four THF molecules coordinating to the lanthanide center with complex **2c** crystallizing with an additional THF molecule in the asymmetric unit. The five-membered rings of **2a–c** all engage in envelope conformations with one of the SiMe_2 units on the flap with distances of 0.73 Å for **2a**, 0.56 Å for **2b**, and 0.78 Å for **2c** from the ring plane.

Compounds **4a** and **4c** (Figure 2) crystallize in the orthorhombic space group $Pbcn$ with three THF molecules coordinating to the lanthanide atoms. The asymmetric units consist of half a molecule, with the Yb or Sm atoms and one oxygen atom of a THF molecule residing on a symmetry plane. The europium compound **4b** crystallizes in the space group $Pna2_1$ but with the whole molecule in the asymmetric unit. The packing patterns of **4a** and **4c** are identical whereas that of the europium compound **4b** is different.

The Si–Yb bond distances in **2a** (3.106 and 3.171 Å) and **4a** (3.0644 Å) are in good agreement with published Cp-free Yb(II) complexes where the distances range from 3.039 to 3.191 Å.^{14,27,29–31} The bond distances of the Eu–Si bonds in **2b** (3.2052, 3.2162 Å) and **4b** (3.1497 Å) are comparable to that found in $\text{Cp}^*\text{Eu}^{\text{II}}\text{SiH}_3\text{K}(\text{THF})_2$ (3.239 Å).¹³ For **2c** (3.2132 and 3.2444 Å) and **4c** (3.1716 Å) the Si–Sm distances are in good agreement with the few published Sm(III)–Si bond lengths (3.133, 3.106, and 3.174 Å)⁹ and the known Sm(II)-silylene complexes (3.189¹⁰ and 3.299¹¹ Å). In general compounds **4a–c** with the two bulky tris(trimethylsilyl)silyl

groups exhibit the shorter bond lengths compared to the metallacyclopentasilanes **2a–c**.

There are 490 compounds in the Cambridge Crystallographic Database⁵⁴ bearing a THF molecule coordinating to an Yb atom with an average bond length Yb–O of 2.386 Å. For the Sm–O bond, this value is 2.510 Å out of 350 examples, and for the Eu–O bond the average distance is 2.565 Å out of 90 examples. In these ranges, all of our compounds fit well. The Si–Si distances also are in all four compounds within the expected range. The bond angles Si–Ln–Si vary only slightly within both the metallacyclopentasilanes **2a–c** (2.76°) and the bis[tris(trimethylsilyl)silyl] derivatives **4a–c** (1.98°). Due to the bulkiness of the two tris(trimethylsilyl)silyl groups the space for coordinating THF molecules is diminished from four for **2a–c** to three in **4a–c**.

Theoretical Studies. The electronic structures of **2a–c** and **4a–c** were calculated at the B3PW91/Basis1 level of theory. This methodology yields an adequate description of the electronic structure of f -block-silyl complexes as was shown in a previous study.¹¹ Table 1 lists the calculated average Ln–Si

Table 1. Calculated Average Ln–Si Bond Lengths (Å), Mayer Bond Orders (MBOs) of Ln–Si Bonds, Natural Population Analysis Charges, and HOMO Energies (eV) for **2a–c** and **4a–c** at B3PW91/Basis1 Level of Theory

compd	Ln–Si bond distance (Å)	MBOs of Ln–Si bonds	NPA charges (Ln/Si)	HOMO energy (eV)
2a	3.145	0.38	+1.76/–0.83	–3.40
2b	3.217	0.32	+1.41/–0.76	–3.36
2c	3.230	0.31	+1.39/–0.76	–3.23
4a	3.076	0.41	+1.71/–0.87	–3.74
4b	3.158	0.37	+1.47/–0.82	–3.65
4c	3.176	0.36	+1.46/–0.80	–3.48

bond lengths (Å), Mayer-bond order (MBO) of Ln–Si bonds, Natural Population Analysis charges, and HOMO energies (eV) for **2a–c** and **4a–c**. These data are in excellent agreement with experimental bond lengths (see Table 1), again confirming the appropriateness of our method of choice. The electronic structures of complexes containing the same lanthanide centers are similar to each other in the sense that they have the same number of unpaired f electrons (0, 7, and 6 for structures **a**, **b**, and **c**, respectively). Natural Population Analysis (NPA) reveals strong ionic character of Ln–Si bonds, with the silicon atoms possessing almost a clear extra electron (Table 1) as NPA charges range between –0.77 and –0.83 while Ln centers have large positive charges (+1.39 to +1.76). Mayer Bond Orders (MBOs) are relatively low (~0.3) similar to our examples of Sm^{II} -silylene complexes, which also show almost zero covalent character, though there is some trend between bond lengths and bond orders.¹¹ HOMO orbitals of **2a–c** and **4a–c** support our analysis (Figure 3 and Supporting Information Figures S26 and S27) as they resemble lone pairs situated on silicon centers with no extension toward the lanthanide centers.

CONCLUSION AND SUMMARY

The chemistry of silyl lanthanides is still a poorly investigated field of research. In the current study we reported a number of lanthanide (+II) complexes with oligosilanyl ligands. The formation of these compounds occurs in a surprisingly facile way by reactions of LnI_2 (Ln = Yb, Eu, Sm) either with a 1,4-oligosilanyl dianion $[\text{K-Si}(\text{SiMe}_3)_2\text{SiMe}_2\text{SiMe}_2\text{Si}(\text{SiMe}_3)_2\text{-K}]$

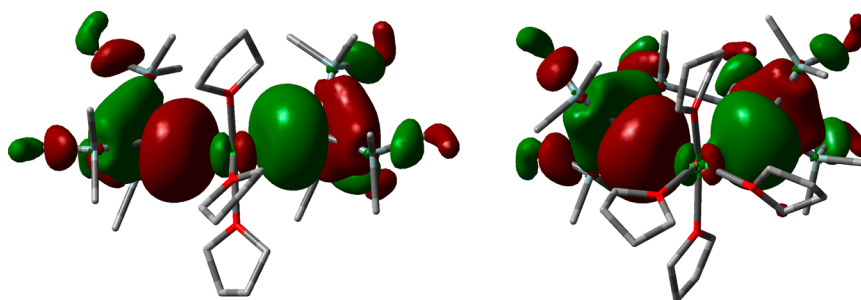


Figure 3. HOMO orbitals of **4a** and **2a**, from left to the right, calculated at B3PW91/Basis1 level of theory (isovalue: 0.02). White, gray, blue, red, and teal colors refer to hydrogen, carbon, oxygen, ytterbium, and silicon atoms, respectively.

(**1**) or with $(\text{Me}_3\text{Si})_3\text{SiK}$ (**3**) to give either the corresponding neutral metallacyclopentasilanes ($\{\text{Me}_2\text{Si}(\text{Me}_3\text{Si})_2\text{Si}\}_2\text{Ln}(\text{THF})_4$ (Ln = Yb (**2a**), Eu (**2b**), Sm (**2c**)) or the neutral disilylated complexes ($\{\text{Me}_3\text{Si}\}_3\text{Si}\}_2\text{Ln}(\text{THF})_3$ (Ln = Yb (**4a**), Eu (**4b**), Sm (**4c**)). While the NMR spectra of the samarium complexes **2c** and **4c** display the extreme chemical shifts typical for paramagnetic compounds, the spectra of the diamagnetic Yb complexes **2a** and **4a** provide useful insight into the electronic situation, revealing strongly shielded resonances consistent with rather anionic silyl units. This picture is also supported by DFT calculations, which were carried for complexes **2a–c** and **4a–c** to elucidate the bonding situation between the Ln(+II) centers and Si. The calculated HOMOs of the complexes resemble very much electron lone pairs at the silicon atoms attached to the metal. The ionic character of the compounds is also exemplified by a reaction of the ytterbacyclopentasilane **2a** with zirconocene dichloride, which smoothly proceeded to the respective zirconacyclopentasilane.

EXPERIMENTAL SECTION

General Remarks. All reactions involving air sensitive compounds were carried out under an atmosphere of dry nitrogen or argon using either Schlenk techniques or a glovebox. All solvents were dried using a column based solvent purification system.⁵⁵ Chemicals were obtained from different suppliers and used without further purification. $[\text{Me}_2\text{Si}(\text{Me}_3\text{Si})_2\text{SiK}]_2$ (**1**)^{40,41} and $(\text{Me}_3\text{Si})_3\text{SiK}$ (**3**)³⁵ were prepared following reported procedures. $\text{SmI}_2 \cdot (\text{THF})_2$, $\text{YbI}_2 \cdot (\text{THF})_2$, and $\text{EuI}_2 \cdot (\text{THF})_2$ were prepared by treatment of the metals in THF with 1,2-diiodoethane.^{32,33,56} Elemental analysis was carried out using a Heraeus VARIO ELEMENTAR instrument.

NMR Spectroscopy. ^1H (300 MHz), ^{13}C (75.4 MHz), and ^{29}Si (59.3 MHz) NMR spectra were recorded on a Varian INOVA 300 spectrometer. To compensate for the low isotopic abundance of ^{29}Si the INEPT pulse sequence was used where possible for the amplification of the signal.^{57,58} To obtain reliable ^1H , ^{13}C , and ^{29}Si NMR shifts, samples with tetramethylsilane (TMS) added were used to obtain a reference point. gHMBC ^1H – ^{29}Si experiments (without TMS added) were carried out to determine all ^{29}Si NMR shifts.

Fluorescence Spectroscopy. The fluorescence of solid compounds **4b** and $\text{EuI}_2(\text{THF})_2$ was recorded with a PerkinElmer LS55 fluorescence spectrometer equipped with a Xe flash lamp as the light source. The solid compound was transferred to the instrument's solid sample holder in the glovebox and kept under nitrogen atmosphere until the sample holder was introduced to the sample chamber of the spectrometer.

X-ray Structure Determination. For X-ray structure analyses the crystals were mounted onto the tip of glass fibers. Data collection was performed with a BRUKER-AXS SMART APEX CCD diffractometer using graphite-monochromated Mo $K\alpha$ radiation (0.710 73 Å). The data were reduced to F^2 and corrected for absorption effects with SAINT⁵⁹ and SADABS,^{60,61} respectively. The structures were solved by direct methods and refined by full-matrix least-squares method

(SHELXL97).⁶² If not noted otherwise all non-hydrogen atoms were refined with anisotropic displacement parameters. All hydrogen atoms were located in calculated positions to correspond to standard bond lengths and angles. Crystallographic data (excluding structure factors) for the structures of compounds **2a**, **2b**, **2c**, **4a**, **4b**, and **4c** reported in this paper have been deposited with the Cambridge Crystallographic Data Center as supplementary publication nos. CCDC-1062936 (**2a**), 1062935 (**2b**), 1026159 (**2c**), 1062933 (**4a**), 1042934 (**4b**), and 1026158 (**4c**). Copies of data can be obtained free of charge at <http://www.ccdc.cam.ac.uk/products/csd/request/>. Figures of solid state molecular structures were generated using Ortep-3 as implemented in WINGX⁶³ and rendered using POV-Ray 3.6.⁶⁴

DFT calculations were carried out by using the GAUSSIAN 09 program.⁶⁵ Geometry optimization was performed with the B3PW91 functional,^{66–68} since it was effectively applied for analogous f-block element-carbene complexes.⁶⁹ We employed the Stuttgart RSC 1997 ECP⁶⁹ basis set from Basis Set Exchange^{70,71} for lanthanide atoms and 6-31G(d)⁷² for Si atoms and 6-31G(d)^{73,74} basis for the other atoms, denoted as Basis1 in the manuscript. Natural Population Analysis was performed with NBO program 5.0^{75–77} implemented in Gaussian 09.

Five-Membered Yb–Si-Complex-(THF)₄ (2a). The reaction was done under strict exclusion of light. To a solution of $\text{YbI}_2 \cdot (\text{THF})_2$ (114 mg, 0.20 mmol) in toluene (4 mL) was added **1** (0.20 mmol, in 2 mL toluene) dropwise. The completeness of the reaction was confirmed after 15 min by ^{29}Si and ^1H NMR. To remove insoluble salts the mixture was filtered over Celite and rewash with toluene (3 mL). After the solvent was removed a dark orange oil was obtained. Crystallization (pentane (15 mL), -37°C , for several days) afforded **2a** (91%, NMR) as orange crystals. Mp: 146–148 °C. NMR (C_6D_6) δ in ppm ^1H : 3.57 (bs, 16H, THF), 1.38 (bs, 16H, THF), 0.76 (s, 12H, SiMe_2), 0.56 (s, 36H, SiMe_3). ^{13}C : 68.4 (THF), 25.3 (THF), 7.4 (SiMe_3), 2.0 (SiMe_2). ^{29}Si : -3.5 ($^2J_{\text{Yb-Si}} = 20$ Hz, SiMe_3), -30.5 (SiMe_2), -154.0 (Si_q). When the reaction was carried out in C_6D_6 instead of toluene with an approximate THF concentration of 9 equiv per Yb, the ^{29}Si NMR spectrum indicated a higher degree of shielding of the metalated silicon atom. NMR (C_6D_6) δ in ppm ^{29}Si : -3.3 ($^2J_{\text{Yb-Si}} = 21$ Hz, SiMe_3), -29.1 (SiMe_2), -163.9 ($^1J_{\text{Yb-Si}} = 633$ Hz, Si_q).

Yb–Si-Complex-(DME)_{1.5}. This involved the same procedure as above only using DME instead of THF as the solvent. NMR (C_6D_6) δ in ppm ^1H : 3.26 (s, 9H, DME), 2.95 (s, 6H, DME), 0.67 (s, 12H, SiMe_2), 0.49 (s, 36H, SiMe_3). ^{13}C : 70.5 (DME), 59.7 (DME), 7.3 (SiMe_3), 1.8 (SiMe_2). ^{29}Si : -2.9 ($^2J_{\text{Yb-Si}} = 20.4$ Hz, SiMe_3), -29.8 (SiMe_2), -158.4 ($^1J_{\text{Yb-Si}} = 656$ Hz, Si_q).

Five-Membered Eu–Si-Complex-(THF)₄ (2b). The same procedure as that for **2a** was used except with **1** (0.16 mmol) and $\text{EuI}_2 \cdot (\text{THF})_2$ (90 mg, 0.16 mmol). Yellow crystals of **2b** (93 mg, 63%) were obtained from pentane at -37°C after several days. Mp: 117–120 °C.

Five-Membered Sm–Si-Complex-(THF)₄ (2c). The same procedure as that for **2a** was used except with $\text{SmI}_2 \cdot (\text{THF})_2$ (288 mg, 0.525 mmol) and **1** (0.500 mmol) in THF and 6 h reaction time. The toluene extract was concentrated to 10 mL and stored at -35°C for 2 days affording green crystals of **2c** (167 mg, 37%). Mp 170–173 °C. NMR (δ in ppm in C_6D_6) ^1H : 4.60 (bs, 16H, THF), 0.65 (bs, 16H, THF), 0.53 (s, 36H, SiMe_3), -1.23 (s, 12H, SiMe_2). ^{13}C : 127.32

(THF), 25.35 (THF), -14.49 (SiMe₂), -18.20 (SiMe₃). ²⁹Si: 120.9 (SiMe₂), -98.3 (SiMe₃), -121.1 (Si_q). Anal. Calcd For C₃₂H₈₀SmO₄Si₈ [904.34]: C 42.52, H 8.92. Found: C 42.33, H 8.32. Anal. Calcd For C₃₂H₈₀SmO₄Si₈ [904.34]: C 42.52, H 8.92. Found: C 42.33, H 8.32.

Bis[tris(trimethylsilyl)silyl]ytterbium·(THF)₃ (4a). The same procedure as that for 2a was used except with 3 (0.31 mmol) and YbI₂·(THF)₂ (89 mg, 0.16 mmol). Yellow-orange crystals of 4a (98 mg, 71%) were obtained from pentane at -37 °C after 24 h. Mp: 154–157 °C. NMR (δ in ppm in C₆D₆) ¹H: 3.62 (bs, 12H, THF), 1.33 (bs, 12H, THF), 0.48 (s, 54H, SiMe₃). ¹³C: 68.2 (THF), 24.7 (THF), 6.3 (SiMe₃). ²⁹Si: -5.3 (²J_{Yb-Si} = 41 Hz, SiMe₃), -144.8 (¹J_{Yb-Si} = 729 Hz, Si_q).

Bis[tris(trimethylsilyl)silyl]europium·(THF)₃ (4b). The same procedure as that for 2a was used except with 3 (0.31 mmol) and EuI₂·(THF)₂ (86 mg, 0.16 mmol). Yellow-orange crystals of 4b (92 mg, 68%) were obtained from pentane at -37 °C after several days. Mp: 156–158 °C.

Bis[tris(trimethylsilyl)silyl]samarium·(THF)₃ (4c). SmI₂·(THF)₂ (290 mg, 0.525 mmol) was dissolved in THF (10 mL), and 3 (0.500 mmol) in THF (6 mL) was added dropwise. The reaction mixture was stirred for 24 h. The solvent was removed under reduced pressure and the residue extracted with pentane (4 times 10 mL) leaving a gray precipitate. The solvent was removed and the residue dissolved in a minimum amount of THF, layered with pentane, and stored at -35 °C for 24 h affording red crystals of 4c (190 mg, 44%). Mp: 150–153 °C. NMR (δ in ppm in C₆D₆) ¹H: 3.17 (bs, 16H, THF), 0.04 (s, 72H, SiMe₃), -0.90 (bs, 16H, THF). ¹³C: 127.20 (THF), 21.81 (THF), -13.40 (SiMe₃). ²⁹Si: -27.4 (SiMe₃), not detected (Si_q). Anal. Calcd For C₃₀H₇₈SmO₃Si₈ [862.33]: C 41.80, H 9.12. Found: C 41.34, H 8.89.

■ ASSOCIATED CONTENT

■ Supporting Information

Tables and CIF files containing crystallographic information for compounds 2a–c and 4a–c, NMR spectra of compounds 2a,c and 4a,c, fluorescence spectra of compound 4b and EuI₂(THF)₂, and tables of Cartesian coordinates and absolute energies for all the complexes studied. The Supporting Information is available free of charge on the ACS Publications website at DOI: 10.1021/acs.inorgchem.5b01072.

■ AUTHOR INFORMATION

■ Corresponding Authors

*E-mail: szilvasitibor@ch.bme.hu.

*E-mail: baumgartner@tugraz.at.

■ Notes

The authors declare no competing financial interest.

■ ACKNOWLEDGMENTS

Support for this study was provided by the Austrian Fonds zur Förderung der wissenschaftlichen Forschung (FWF) via projects P-25124 (J.B.) and P-26417 (C.M.). T.S. is thankful for the generous support by The New Széchenyi Plan TÁMOP-4.2.2/B-10/1-2010-0009.

■ REFERENCES

- Bochkarev, M. N. *Coord. Chem. Rev.* **2004**, *248*, 835–851.
- Evans, W. J. *Coord. Chem. Rev.* **2000**, *206–207*, 263–283.
- MacDonald, M. R.; Ziller, J. W.; Evans, W. J. *J. Am. Chem. Soc.* **2011**, *133*, 15914–15917.
- MacDonald, M. R.; Bates, J. E.; Fieser, M. E.; Ziller, J. W.; Furche, F.; Evans, W. J. *J. Am. Chem. Soc.* **2012**, *134*, 8420–8423.
- MacDonald, M. R.; Bates, J. E.; Ziller, J. W.; Furche, F.; Evans, W. J. *J. Am. Chem. Soc.* **2013**, *135*, 9857–9868.

- Fieser, M. E.; MacDonald, M. R.; Krull, B. T.; Bates, J. E.; Ziller, J. W.; Furche, F.; Evans, W. J. *J. Am. Chem. Soc.* **2015**, *137*, 369–382.
- Radu, N. S.; Tilley, T. D.; Rheingold, A. L. *J. Am. Chem. Soc.* **1992**, *114*, 8293–8295.
- Radu, N. S.; Tilley, T. D.; Rheingold, A. L. *J. Organomet. Chem.* **1996**, *516*, 41–49.
- Radu, N. S.; Hollander, F. J.; Tilley, T. D.; Rheingold, A. L. *Chem. Commun.* **1996**, 2459–2460.
- Evans, W. J.; Perotti, J. M.; Ziller, J. W.; Moser, D. F.; West, R. *Organometallics* **2003**, *22*, 1160–1163.
- Zitz, R.; Arp, H.; Hlina, J.; Walewska, M.; Marschner, C.; Szilvási, T.; Blom, B.; Baumgartner, J. *Inorg. Chem.* **2015**, *54*, 3306–3315.
- Corradi, M. M.; Frankland, A. D.; Hitchcock, P. B.; Lappert, M. F.; Lawless, G. A. *Chem. Commun.* **1996**, 2323–2324.
- Hou, Z.; Zhang, Y.; Nishiura, M.; Wakatsuki, Y. *Organometallics* **2003**, *22*, 129–135.
- Bochkarev, L. N.; Makarov, V. M.; Hrzhanovskaya, Y. N.; Zakharov, L. N.; Fukin, G. K.; Yanovsky, A. I.; Struchkov, Y. T. *J. Organomet. Chem.* **1994**, *467*, C3–C5.
- Booij, M.; Kiers, N. H.; Heeres, H. J.; Teuben, J. H. *J. Organomet. Chem.* **1989**, *364*, 79–86.
- Eppinger, J.; Spiegler, M.; Hieringer, W.; Herrmann, W. A.; Anwander, R. *J. Am. Chem. Soc.* **2000**, *122*, 3080–3096.
- Anwander, R.; Runte, O.; Eppinger, J.; Gerstberger, G.; Herdtweck, E.; Spiegler, M. *J. Chem. Soc., Dalton Trans.* **1998**, 847–858.
- Corey, J. Y. *Chem. Rev.* **2011**, *111*, 863–1071.
- Gountchev, T. I.; Tilley, T. D. *Organometallics* **1999**, *18*, 5661–5667.
- Wang, Q.; Xiang, L.; Song, H.; Zi, G. *Inorg. Chem.* **2008**, *47*, 4319–4328.
- Qian, C.; Nie, W.; Chen, Y.; Sun, J. *J. Organomet. Chem.* **2002**, *645*, 82–86.
- Fang, M.; Farnaby, J. H.; Ziller, J. W.; Bates, J. E.; Furche, F.; Evans, W. J. *J. Am. Chem. Soc.* **2012**, *134*, 6064–6067.
- Scherer, W.; McGrady, G. S. *Angew. Chem., Int. Ed.* **2004**, *43*, 1782–1806.
- Saßmannshausen, J. *Dalton Trans.* **2012**, *41*, 1919–1923.
- Perrin, L.; Maron, L.; Eisenstein, O.; Lappert, M. F. *New J. Chem.* **2003**, *27*, 121–127.
- Brady, E. D.; Clark, D. L.; Gordon, J. C.; Hay, P. J.; Keogh, D. W.; Poli, R.; Scott, B. L.; Watkin, J. G. *Inorg. Chem.* **2003**, *42*, 6682–6690.
- Chen, Y.; Song, H.; Cui, C. *Angew. Chem., Int. Ed.* **2010**, *49*, 8958–8961.
- Niemeyer, M. In *Organosilicon Chemistry IV*; Auner, N., Weis, J., Eds.; Wiley-VCH: New York, 2005; pp 323–329.
- Niemeyer, M. *Inorg. Chem.* **2006**, *45*, 9085–9095.
- Yan, K.; Upton, B. M.; Ellern, A.; Sadow, A. D. *J. Am. Chem. Soc.* **2009**, *131*, 15110–15111.
- Yan, K.; Schoendorff, G.; Upton, B. M.; Ellern, A.; Windus, T. L.; Sadow, A. D. *Organometallics* **2013**, *32*, 1300–1316.
- Girard, P.; Namy, J. L.; Kagan, H. B. *J. Am. Chem. Soc.* **1980**, *102*, 2693–2698.
- Synthetic Methods of Organometallic and Inorganic Chemistry*; Herrmann, W. A., Brauer, G., Eds.; Georg Thieme Verlag; Thieme Medical Publishers: Stuttgart, 1996.
- Gaderbauer, W.; Zirngast, M.; Baumgartner, J.; Marschner, C.; Tilley, T. D. *Organometallics* **2006**, *25*, 2599–2606.
- Kayser, C.; Fischer, R.; Baumgartner, J.; Marschner, C. *Organometallics* **2002**, *21*, 1023–1030.
- Orudjeva, K. N.; Suleymanov, Y. Z. *Kim. Probl. J.* **2003**, 93–96.
- Zirngast, M.; Flörke, U.; Baumgartner, J.; Marschner, C. *Chem. Commun.* **2009**, 5538–5540.
- Sgro, M. J.; Piers, W. E. *Inorg. Chim. Acta* **2014**, *422*, 243–250.
- Fischer, R.; Konopa, T.; Baumgartner, J.; Marschner, C. *Organometallics* **2004**, *23*, 1899–1907.

- (40) Fischer, R.; Frank, D.; Gaderbauer, W.; Kayser, C.; Mechtler, C.; Baumgartner, J.; Marschner, C. *Organometallics* **2003**, *22*, 3723–3731.
- (41) Kayser, C.; Kickelbick, G.; Marschner, C. *Angew. Chem., Int. Ed.* **2002**, *41*, 989–992.
- (42) Farwell, J. D.; Lappert, M. F.; Marschner, C.; Strissel, C.; Tilley, T. D. *J. Organomet. Chem.* **2000**, *603*, 185–188.
- (43) Kayser, C.; Frank, D.; Baumgartner, J.; Marschner, C. *J. Organomet. Chem.* **2003**, *667*, 149–153.
- (44) Frank, D.; Baumgartner, J.; Marschner, C. *Chem. Commun.* **2002**, 1190–1191.
- (45) Arnold, J.; Tilley, T. D.; Rheingold, A. L.; Geib, S. J. *Inorg. Chem.* **1987**, *26*, 2106–2109.
- (46) Gaderbauer, W.; Balatoni, I.; Wagner, H.; Baumgartner, J.; Marschner, C. *Dalton Trans.* **2010**, *39*, 1598.
- (47) Schumann, H.; Nickel, S.; Hahn, E.; Heeg, M. J. *Organometallics* **1985**, *4*, 800–801.
- (48) Evans, W. J.; Gonzales, S. L.; Ziller, J. W. *J. Am. Chem. Soc.* **1991**, *113*, 7423–7424.
- (49) Evans, W. J.; Bloom, I.; Hunter, W. E.; Atwood, J. L. *J. Am. Chem. Soc.* **1981**, *103*, 6507–6508.
- (50) Meijerink, A.; Nuyten, J.; Blasse, G. *J. Lumin.* **1989**, *44*, 19–31.
- (51) Wang, X.; Zhao, Z.; Wu, Q.; Li, Y.; Wang, C.; Mao, A.; Wang, Y. *Dalton Trans.* **2015**, *44*, 11057–11066.
- (52) Deng, D.; Yu, H.; Li, Y.; Hua, Y.; Jia, G.; Zhao, S.; Wang, H.; Huang, L.; Li, Y.; Li, C.; Xu, S. *J. Mater. Chem. C* **2013**, *1*, 3194–3199.
- (53) Rogers, E.; Dorenbos, P.; de Haas, J. T. M.; van der Kolk, E. J. *Phys.: Condens. Matter* **2012**, *24*, 275502.
- (54) Conquest Version 1.16 was used: Bruno, I. J.; Cole, J. C.; Edgington, P. R.; Kessler, M.; Macrae, C. F.; McCabe, P.; Pearson, J.; Taylor, R. *Acta Crystallogr., Sect. B* **2002**, *58*, 389–397.
- (55) Pangborn, A. B.; Giardello, M. A.; Grubbs, R. H.; Rosen, R. K.; Timmers, F. J. *Organometallics* **1996**, *15*, 1518–1520.
- (56) Evans, W. J.; Grate, J. W.; Choi, H. W.; Bloom, I.; Hunter, W. E.; Atwood, J. L. *J. Am. Chem. Soc.* **1985**, *107*, 941–946.
- (57) Morris, G. A.; Freeman, R. *J. Am. Chem. Soc.* **1979**, *101*, 760–762.
- (58) Helmer, B. J.; West, R. *Organometallics* **1982**, *1*, 877–879.
- (59) SAINTPLUS: *Software Reference Manual, Version 6.45*; Bruker-AXS: Madison, WI, 1997–2003.
- (60) Blessing, R. H. *Acta Crystallogr., Sect. A* **1995**, *51*, 33–38.
- (61) Sheldrick, G. M. *SADABS, Version 2.10*; Bruker AXS Inc.: Madison, WI, 2003.
- (62) Sheldrick, G. M. *Acta Crystallogr., Sect. A* **2008**, *64*, 112–122.
- (63) Farrugia, L. J. *J. Appl. Crystallogr.* **2012**, *45*, 849–854.
- (64) POVRAY 3.6. *Persistence of Vision Pty. Ltd.*; 2004. Retrieved from <http://www.povray.org/download/>.
- (65) Frisch, M. J.; Trucks, G. W.; Cheeseman, J. R.; Scalmani, G.; Caricato, M.; Hratchian, H. P.; Li, X.; Barone, V.; Bloino, J.; Zheng, G.; Vreven, T.; Montgomery, J. A.; Petersson, G. A.; Scuseria, G. E.; Schlegel, H. B.; Nakatsuji, H.; Izmaylov, A. F.; Martin, R. L.; Sonnenberg, J. L.; Peralta, J. E.; Heyd, J. J.; Brothers, E.; Ogliaro, F.; Bearpark, M.; Robb, M. A.; Mennucci, B.; Kudin, K. N.; Staroverov, V. N.; Kobayashi, R.; Normand, J.; Rendell, A.; Gomperts, R.; Zakrzewski, V. G.; Hada, M.; Ehara, M.; Toyota, K.; Fukuda, R.; Hasegawa, J.; Ishida, M.; Nakajima, T.; Honda, Y.; Kitao, O.; Nakai, H. *Gaussian 09*; Gaussian, Inc.: Wallingford, CT, 2009.
- (66) Perdew, J. P. In *Electronic Structure of Solids '91*; Ziesche, P., Eschrig, H., Eds.; Akademie Verlag: Berlin, 1991; pp 11–20.
- (67) Becke, A. D. *J. Chem. Phys.* **1993**, *98*, 5648–5652.
- (68) Burke, K.; Perdew, J. P.; Wang, Y. In *Electronic Density Functional Theory: Recent Progress and New Directions*; Dobson, J. F., Vignale, G., Das, M. P., Eds.; Plenum Press: New York, 1998; pp 81–111.
- (69) Dolg, M.; Stoll, H.; Savin, A.; Preuss, H. *Theor. Chim. Acta* **1989**, *75*, 173–194.
- (70) Feller, D. *J. Comput. Chem.* **1996**, *17*, 1571–1586.
- (71) Schuchardt, K. L.; Didier, B. T.; Elsethagen, T.; Sun, L.; Gurumoorthi, V.; Chase, J.; Li, J.; Windus, T. L. *J. Chem. Inf. Model.* **2007**, *47*, 1045–1052.
- (72) Clark, T.; Chandrasekhar, J.; Spitznagel, G. W.; Schleyer, P. V. *R. J. Comput. Chem.* **1983**, *4*, 294–301.
- (73) Hariharan, P. C.; Pople, J. A. *Theor. Chim. Acta* **1973**, *28*, 213–222.
- (74) Frisch, M. J.; Pople, J. A.; Binkley, J. S. *J. Chem. Phys.* **1984**, *80*, 3265–3269.
- (75) Glendening, E. D.; Badenhoop, J. K.; Reed, A. E.; Carpenter, J. E.; Bohman, J. A.; Morales, C. M.; Weinhold, F. *NBO Version 5.0*, 2001.
- (76) Weinhold, F.; Landis, C. R. *Chem. Educ. Res. Pract.* **2001**, *2*, 91–104.
- (77) Carpenter, J. E.; Weinhold, F. *THEOCHEM* **1988**, *169*, 41–62.